Case Studies in Thermal Engineering 64 (2024) 105422

Contents lists available at ScienceDirect

Case Studies in Thermal Engineering

journal homepage: www.elsevier.com/locate/csite

Optimisation studies on performance enhancement of spray cooling - Machine learning approach

Umesh B. Deshannavar [a], Saee H. Thakur [b], Amith H. Gadagi [c], Santosh A. Kadapure [a], Santhosh Paramasivam [d,*], Natarajan Rajamohan [e,**], Raffaello Possidente [f], Gianluca Gatto [d]

[a] Department of Chemical Engineering, Tatyasaheb Kore Institute of Engineering and Technology, Warana University, Warananagar, India
[b] Department of Biotechnology Engineering, KIT's College of Engineering, Kolhapur, India
[c] Department of Mechanical Engineering, KLE Dr. M. S. Sheshgiri College of Engineering and Technology, Belagavi, India
[d] Department of Electrical and Electronic Engineering, University of Cagliari, Cagliari, Italy
[e] Chemical Engineering Section, Faculty of Engineering, Sohar University, Sohar, Oman
[f] Department of Civil and Environmental Engineering, University of Cagliari, Cagliari, Italy

ARTICLE INFO

Handling Editor: Huihe Qiu

Keywords:
Spray cooling
Heat transfer coefficient
Nozzle inclination angle
Water pressure
Spray height
Machine learning

ABSTRACT

The performance optimisation of spray cooling heat transfer systems has been identified as a significant step in improving process efficiency, and the application of machine learning tools is a recent development that has enhanced this. This study aims to maximise the heat transfer coefficient for spray cooling at low heat flux levels. The effects of nozzle inclination angle, water pressure, and spray height on heat transfer coefficient were studied. Taguchi L_{27} orthogonal array technique was used to perform the experiments. A maximum heat transfer coefficient of 181.4 kW/m^{2}K was obtained at a nozzle inclination angle of 60°, spray height of 4 cm, and water pressure of 15 psi. Analysis of variance was performed to find the significance of each variable and its interactions. The results show that for the maximum heat transfer coefficient (181.4 kW/m^{2}K), the optimum levels of the independent variables were A3H1P3, i.e., the highest level of nozzle inclination angle (60°), the lowest level of spray height (4 cm), and the highest level of water pressure (15 psi). The support vector machine outperformed the Random Forest algorithm and Multiple Regression analysis regarding prediction accuracy with a maximum error of 0.15 % and root mean squared error of 0.01.

1. Introduction

The Industrial Revolution caused a perpetual increase in mechanisation and machinery utilisation. The increase in power density of machinery components has led to equipment durability and stability issues due to excessive heating of devices, which mandates effective cooling techniques by improving heat dissipation.

Traditional cooling systems employ jet impingement, pool boiling, heat pipe, and forced convection to enhance the heat transfer coefficient (HTC) [1–3]. The heat dissipation rate sometimes becomes a barrier to equipment operation and a primary hurdle for the

* Corresponding author. Department of Electrical and Electronic Engineering, University of Cagliari, Cagliari, Italy.
** Corresponding author. Chemical Engineering section, Faculty of Engineering, Sohar University, Sohar, Oman.
E-mail addresses: santhosh.paramasivam@unica.it (S. Paramasivam), rnatarajan@su.edu.om (N. Rajamohan).

https://doi.org/10.1016/j.csite.2024.105422
Received 12 April 2024; Received in revised form 28 October 2024; Accepted 3 November 2024
Available online 5 November 2024

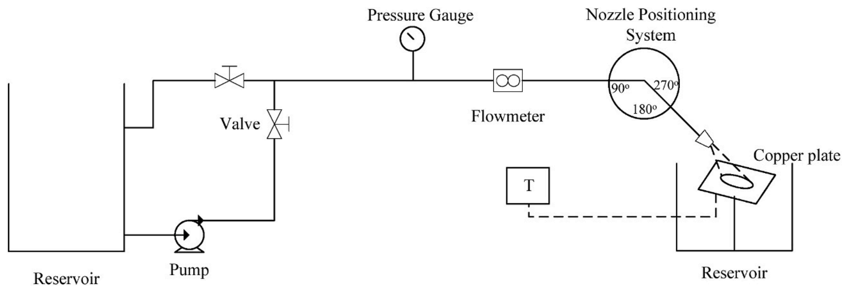

Fig. 1. Schematic diagram of experiment test rig.

production industries [4,5]. In the past decade, spray cooling, a relatively modern and direct technique, has become prevalent for reducing excess heat flux [6,7]. Spray cooling is a promising heat dissipation technique for various applications, including solar panel cooling, fuel cells, and electronic devices. It effectively reduces temperatures, enhances thermal comfort, and improves overall system performance [8–11]. Unlike traditional heat dissipation technologies, spray cooling has several advantages, such as a higher HTC, a greater critical heat flux [12], a low coolant mass flow rate [13], and a more uniform wall temperature [14,15]. Spray cooling can efficiently dissipate high heat fluxes, and its performance is influenced by factors like mass flow rate, nozzle diameter, and spray height [16,17]. Thus extensive studies on spray cooling HTC have been conducted on parameters such as nozzle type [18–20], spray height [21–23], heat transfer surface modification [24–27], spray cooling analysis method [28–30], spray cooling mechanism [31–33], etc.

Cheng et al. [34] examined the effects of spray height and inlet coolant pressure on HTC in spray cooling. Experiments were conducted with distilled water in an open-loop testing system. The findings suggested that an increase in inlet fluid pressure and a decrease in spray height increases the HTC under a low heat flux range.

Gao et al. [35] investigated the effects of nozzle position on spray cooling performance in a full cone nozzle system. The nozzle inclination angle varying from 20 to 40° increased HTC from 2.22 to 3.01 W/cm^{2}K. Azzam et al. [36,37] used deionised water as the coolant to examine the effects of spray parameters on cooling. The results of 10 mm spray height and inlet water pressure in the range of 78.6–183.515 kPa showed that increased pressure increases the atomisation and droplet velocity and hence the enhancement of HTC in plane surfaces [38,39]. Hong et al. [40,41] investigated spray cooling heat transfer characteristics with distilled water as a cooling medium and concluded that smaller droplet size leads to thicker wall films and higher HTCs in low heat flux conditions. Also, the literature reports the effects of spray height, spray incidence and nozzle inclination angles, and water pressure at the inlet on spray cooling heat transfer [42,43]. Hocine et al. [44] studied the effect of water spray pressure in the 1–4 bars range on a heated beryllium-copper alloy plate between the temperature range of 100–815 °C. The results demonstrated that the HTC ranges from 9000 to 39000 W/m^{2}K, which proved the effectiveness of an increase in spray pressure on enhanced heat transfer performance.

Based on the heat-transfer mode on a spray-covered hot surface, spray cooling can be categorised into three regimes: the single-phase regime, the two-phase regime, and the critical heat flux (CHF). A comprehensive literature database exists to understand heat transfer mechanisms in these various regimes and the effects of coolants, surface characteristics, and nozzle types on high heat flux applications. Research on spray cooling heat transfer applications in high and medium heat flux zones is reported [45–47]. On the other hand, spray liquid cooling studies in low heat flux zones provide much room for further research. A comprehensive literature review on cooling techniques revealed a knowledge gap regarding the precise heat transfer mechanisms in low heat flux zones. This research aims to address this deficiency by investigating the influence of spray properties on heat transfer in these regions. Specifically, the study will explore the possibility of achieving uniform surface temperatures and predicting heat transfer coefficients for low heat flux applications. A computational model is required to predict heat transfer coefficients (HTC) for spray cooling applications in low heat flux zones. This research studied heat transfer under single-phase conditions in a low heat flux zone. To bridge this gap, we investigated optimal conditions for using a full cone nozzle at various nozzle inclination angles, water pressures, and spray heights. Taguchi's L_{27} orthogonal array approach was employed to experiment on the effects of three factors at three levels. Data analysis was performed for experimental results using Minitab software. Variance (ANOVA) analysis was conducted to determine the significance of each independent spray variable and their interactions. Machine learning models, specifically Random Forest and support vector machine algorithms, were developed to predict the heat transfer coefficient (HTC) for spray cooling.

2. Experimental design

2.1. Experiment test rig

The experiment test rig depicted in Fig. 1 and photograph in Plate 1 consists of a nozzle, a copper plate, a flow measurement device, and a pump. The copper plate (10-inch × 10-inch) is provided with an electrical heating coil and six *K*-type thermocouples attached parallelly, three in each layer beneath the copper plate, 2.5 inches apart. The thermocouples are further coupled with the data acquisition system. The nozzle positioning system (NPS) is provided to adjust the inclination angle and orientation of the nozzle. A customised Arduino flow meter and a pressure gauge are provided to measure the volumetric flow rate and pressure. A bypass valve is provided to adjust the flow rate. A high-speed camera (NIKON D5200) records the spray pattern (Plate 2). The inlet and outlet

Table 1
Taguchi L_{27} experimental design and results for spray cooling.

Run	Nozzle inclination angle (deg)	Spray height (cm)	Inlet water pressure (psi)	HTC (kW/m^2K)	S/N ratio (dB)
1	30	4	5	92.48	39.32
2	30	4	10	103.39	40.29
3	30	4	15	120.88	41.65
4	30	5	5	84.28	38.51
5	30	5	10	95.75	39.62
6	30	5	15	115.11	41.22
7	30	6	5	68.82	36.75
8	30	6	10	83.12	38.39
9	30	6	15	101.95	40.17
10	45	4	5	127.74	42.13
11	45	4	10	143.84	43.16
12	45	4	15	162.48	44.22
13	45	5	5	109.04	40.75
14	45	5	10	125.05	41.94
15	45	5	15	135.54	42.64
16	45	6	5	86.73	38.76
17	45	6	10	106.55	40.55
18	45	6	15	124.36	41.89
19	60	4	5	137.35	42.76
20	60	4	10	154.11	43.76
21	60	4	15	181.37	45.17
22	60	5	5	118.67	41.49
23	60	5	10	134.94	42.60
24	60	5	15	155.56	43.84
25	60	6	5	95.96	39.64
26	60	6	10	128.66	42.19
27	60	6	15	142.27	43.06

temperatures of the coolant water are measured using digital thermometers. An adjustable stand is used to hold the copper plate firmly and to maintain the required spray height.

2.2. Experimentation

The full cone nozzle assembly was attached to the setup, and the required spray height was adjusted using an adjustable stand. The nozzle inclination angle was adjusted with the help of the NPS. The copper plate was heated, the pump was switched on, and the required water inlet pressure and flow rate were adjusted using a bypass valve. The initial temperature of the working fluid was recorded. During the coolant spraying on the hot surface, images were captured, and the droplet size of the water was measured with ImageJ software. The time required for the hot surface to cool down to ambient and exit water temperatures was recorded. The experimental data obtained were analysed for HTC calculations.

2.3. Design of spray cooling experiments

The Taguchi L_{27} fractional factorial design matrix was utilised. Three factors and three levels were considered during the design of the experiments. The impact of variables such as nozzle inclination angle (30, 45, and 60°), inlet water pressure (5, 10, and 15 psi), and spray height (4, 5, and 6 cm) was investigated on HTC. For the Taguchi L_{27} fractional factorial design, each variable's range was decided based on the series of tests conducted over a greater range using the one variable at a time method. Table 1 displays the L_{27} experimental design matrix that optimised factors affecting the HTC and signal-to-noise (S/N) ratio.

As this work involves maximising HTC, the S/N was chosen as "larger is better". S/N ratio is calculated by [48].

$$\frac{S}{N} = -10 \log \left(\frac{1}{n} \sum_{i=1}^{n} \frac{1}{R_i^2} \right) \tag{1}$$

Here n represents the number of repetitions, and R_i is the response (HTC) for the ith experiment.

2.4. Statistical analysis

Minitab 18 software was used to conduct the statistical analysis. ANOVA was used to analyse the Taguchi design's outcomes, and *F*-values were acquired for the created ANOVA test. Then, the significant factors were identified at a 95 % confidence level using these *F*-values and the corresponding *P*- value.

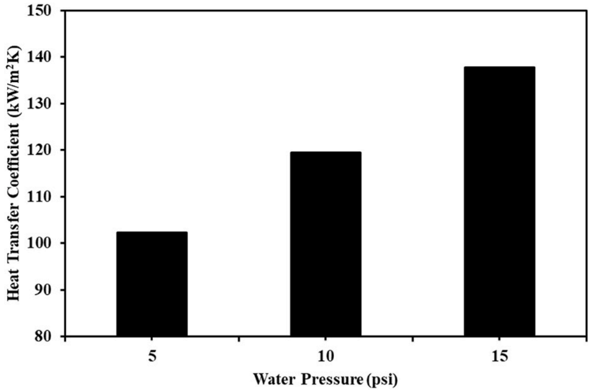

Fig. 2. Effect of water pressure on HTC.

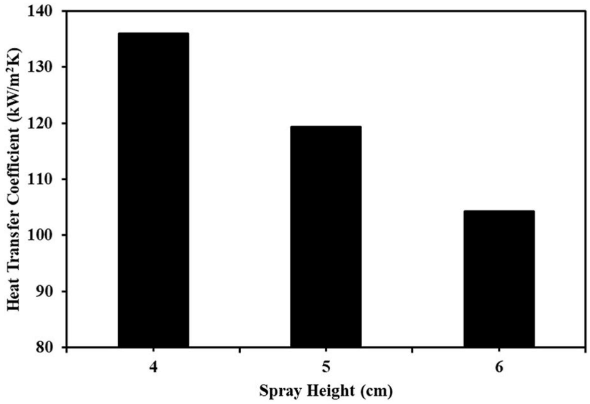

Fig. 3. Effect of spray height on HTC.

3. Results and discussions

3.1. Optimisation

The experiments were carried out following the L_{27} Taguchi design (Table 1) to estimate the HTC. The HTC values range from 68.82 to 181.38 kW/m^{2}K. In order to investigate the effects of individual factors, the average response of individual factors (nozzle inclination angle, spray height, water pressure) on HTC value at various levels derived from the Taguchi L_{27} design was analysed and discussed.

3.2. Water inlet pressure

The HTC increased as the inlet water pressure increased (Fig. 2). This increase in the HTC with an increase in inlet water pressure is attributed to the rise in the impingement density [49]. As inlet water pressure increases, the volumetric flow rate, droplet impact velocity, and number of droplets in the spray also increase [50,51]. At higher impact velocities of a droplet, convective heat transfer becomes strong between the droplet and solid surface; thus, higher heat transfer performance is achieved [52]. In addition to this, an increase in water pressure results in a decrease in droplet size [53]. As droplet size decreases, wall film thickness increases, enhancing convection heat transfer, an influential phenomenon in low heat flux. So, better heat transfer efficiencies were observed with a decrease in droplet size as inlet water pressure increases [54]. Also, when the inlet pressure is increased, the exclusion of bubbles from the liquid film and the heat transfer mechanism is accelerated [55]. The impact of incoming water pressure on the HTC in spray cooling for different situations was also reported by Refs. [56–59].

3.3. Spray height

The HTC decreased as spray height increased (Fig. 3). For greater heights, droplets cover the entire heating surface, whereas, for shorter heights, spray covers only a tiny portion of the heating surface. The heating surface is beneath the dense spray region during the short spray height (4 cm). This increase in HTC at smaller heights is due to the inability of fluid to drain away immediately.

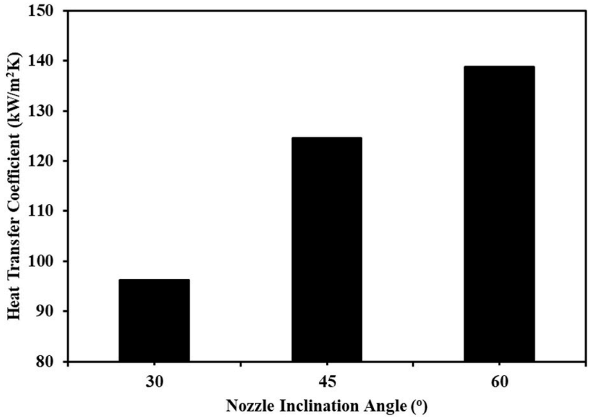

Fig. 4. Effect of nozzle inclination angle on HTC.

Table 2
ANOVA analysis for the effects of nozzle inclination angle, inlet water pressure, and spray height on spray cooling heat transfer co-efficient.

Source	DF[a]	Seq SS[b]	Contribution (%)	Adj SS[c]	Adj MS[d]	*F*-Value	*P*-Value	VIF[e]
Regression	3	18308.6	95.24	18308.6	6102.86	153.40	0.000	
Nozzle inclination angle	1	8154.5	42.42	8154.5	8154.49	204.97	0.000	1.00
Spray height	1	4519.9	23.51	4519.9	4519.86	113.61	0.000	1.00
Inlet water pressure	1	5634.2	29.31	5634.2	5634.22	141.62	0.000	1.00
Error	23	915.0	4.76	915.0	39.78			
Total	26	19223.6	100					

[a] Degree of freedom.
[b] Sequential sum of squares.
[c] Adjusted sum of squares.
[d] Adjusted mean of squares, and.
[e] Variance inflation factor.

Additionally, hitting droplets and incoming droplets from the nozzle combine to form a thin liquid layer that flows outward, covering the whole heating surface. Therefore, cooling of the hot surface is achieved uniformly and effectively [55]. In the case of larger heights, at the centre of the heating plate, a hollow region appears and expands, resulting in decreased droplet momentum and weak liquid film formation. Therefore, at greater spray heights, surface temperature heterogeneity and poor heat transfer performance were observed [55,60]. Tian et al. [61] determined an optimum spray height of 4.31 cm using R404A as a coolant. There is no consensus in the literature on the optimal nozzle-to-surface distance as researchers use a variety of coolants and different experimental conditions. Various researchers have worked on optimising HTC's spray height using different coolants. However, due to the different experimental conditions, the most suitable nozzle-to-surface distances obtained from each experiment are incomparable [62].

3.4. Nozzle inclination angle

In spray cooling studies, nozzle inclination angle plays a vital role. Fig. 4 shows that the nozzle inclination angle increases the HTC. This work conducted experiments by changing the inclination angle and maintaining a constant spray height. While retaining the nozzle inclination angle, one must ensure that the entire surface can get enough cooling medium [63]. The formation of a stagnation zone is one of the reasons for a decrease in heat transfer performance. An increase in nozzle inclination angle ensures washing and reduction in stagnation zone area, which results in high heat transfer performance. At low inclination angles and higher spray heights, spray droplets directly impact a small fraction of the heated area. In addition, liquid spray falls outside the heated area, resulting in the wastage of coolant and lowering heat transfer performance. The optimum value of the inclination angle of a nozzle is the one that ensures maximum contact region, fully utilised spray liquid, and minimum stagnation zone area [64]. Also, it is observed during experimentation that an increase in the inclination angle of the nozzle improves the uniformity of surface temperature distribution, resulting in higher HTC values. Similar observations were made by Gao et al. [65] and Yang et al. [66].

3.5. ANOVA and regression analysis

ANOVA is a statistical tool that finds systematic and random factors inside an experimental data set. The influence of the independent variables on the dependent variable is analysed in a regression study using the ANOVA test. Additionally, this tool divides observed variance data into multiple components that are used for the *F*-test and *P*-test. The adjusted mean of squares (Adj MS), a

Table 3
Taguchi Analysis for ranks of nozzle inclination angle, inlet water pressure, and spray height.

Level	Nozzle inclination angle (*A*)	Spray height (*H*)	Inlet water pressure (*P*)
1	96.20	135.96	102.34
2	124.59	119.33	119.49
3	138.77	104.27	137.73
Delta	42.57	31.69	35.38
Rank	1	3	2

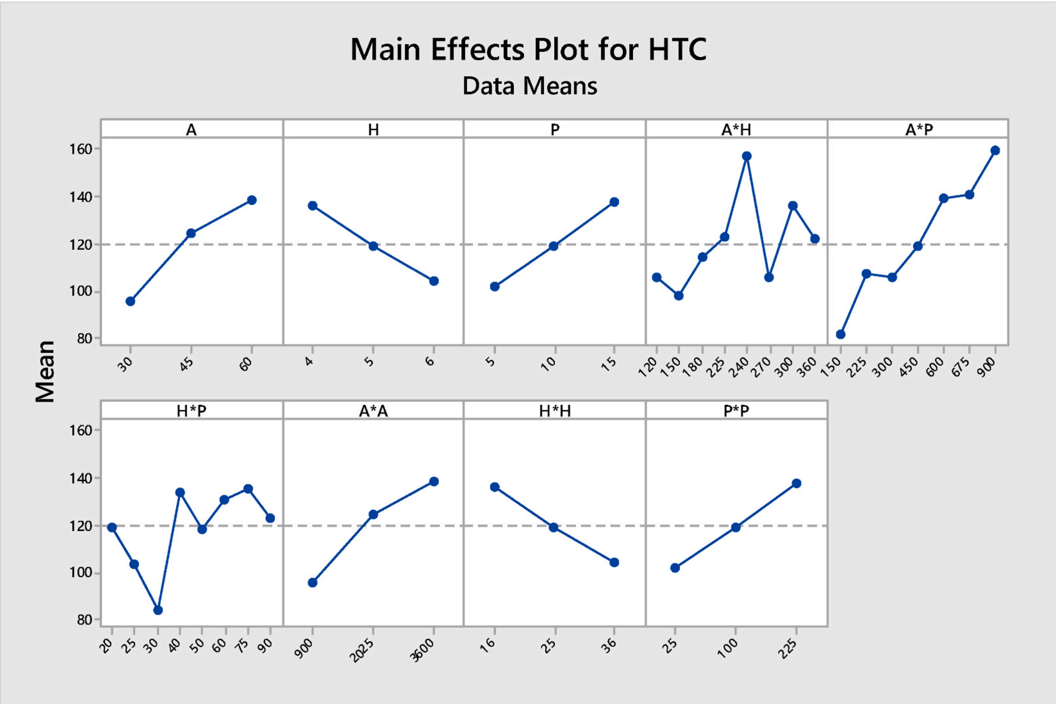

Fig. 5. Main effects plot for means of Spray Cooling process parameters on HTC.

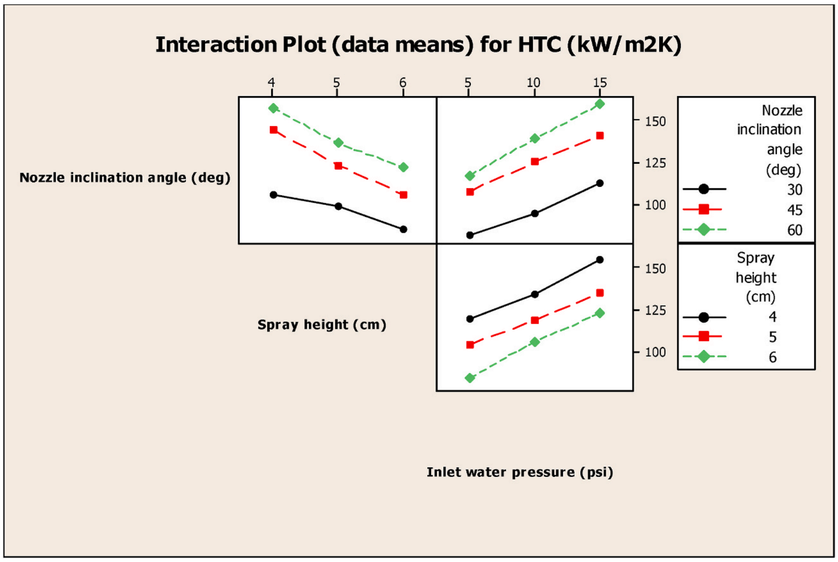

Fig. 6. Interaction plots for coefficient of heat transfer.

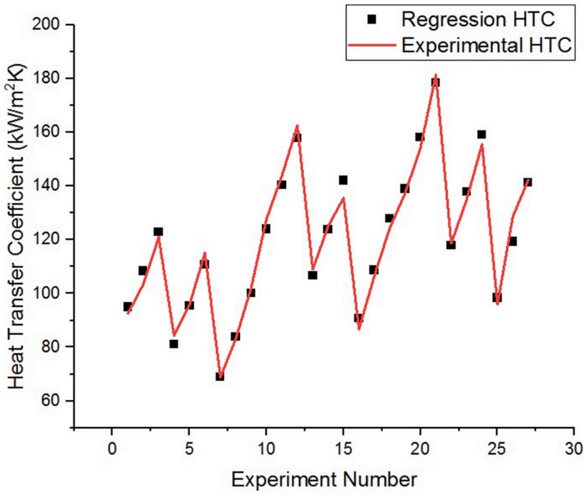

Fig. 7. Comparison of the Regression predicted values vs. the experimental values.

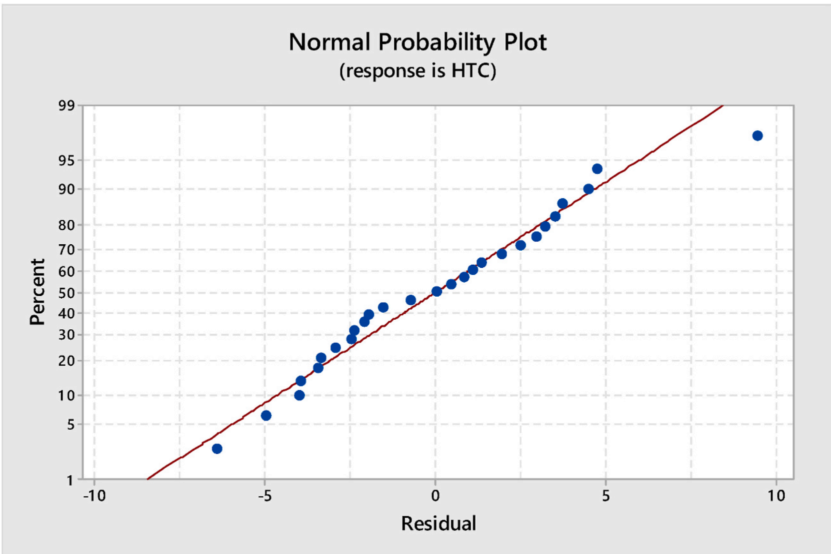

Fig. 8. Normal probability plot of residuals.

sequential sum of squares (Seq SS), an adjusted sum of squares (Adj SS), and degrees of freedom (DF) terms represent measures of variation for different model components and the amount of information in an experimental data set. The ANOVA analysis in Table 2 indicates the effect of factors: nozzle inclination angle, inlet water pressure, and spray height. A high *F*-test value (204.97) suggests that not all group means are equal and that the variability between group means is greater than the variability of the group observations. Each factor's statistical significance is assessed using a *P*-value (<0.05) with a 95 % degree of confidence and the percentage contribution taken from the Seq SS column.

The relative relevance of the spray variables is determined using an ANOVA. It can be deduced that the HTC was significantly influenced by the nozzle inclination angle followed by inlet water pressure and spray height. The percentage contribution of nozzle inclination angle, inlet water pressure, and spray height on HTC was 42.42 %, 29.31 % and 23.51 %, respectively, with a percentage error of 4.76. The variance inflation factor (VIF) of 1 for all the factors suggests no multicollinearity between the independent variables and, hence, no influence on each other in determining the HTC. Table 3 represents the response table for the means and rank of each independent variable. The delta values in Table 3 represent the range between the maximum and minimum heat transfer coefficients for each parameter. These delta values are compared to determine the ranks. The highest delta value (42.57) corresponds to the nozzle inclination angle, assigned Rank 1. The delta values for inlet pressure and spray height are 35.38 and 31.69, respectively, leading to Rank 2 and Rank 3 being assigned to these parameters.

From Table 3 and Fig. 5 it is observed that the optimum levels of independent variables for maximum HTC are, *A*3*H*1*P*3 i.e., the

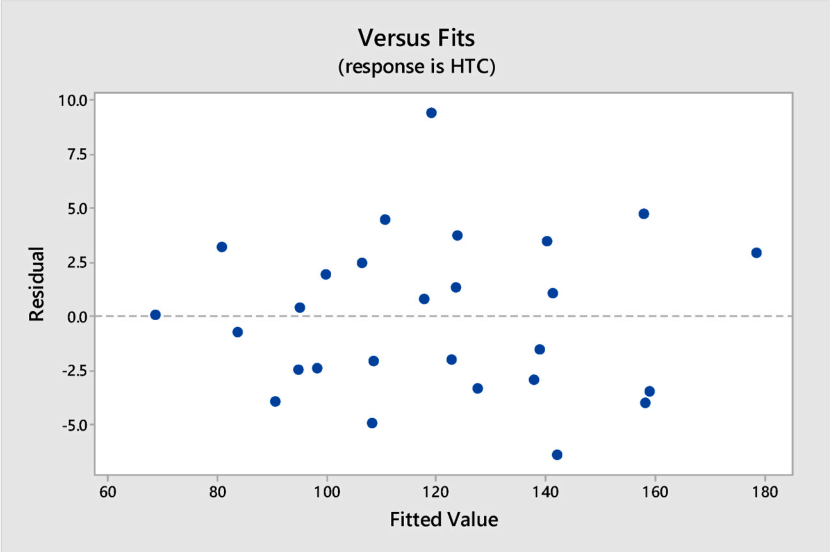

Fig. 9. Distribution of residuals.

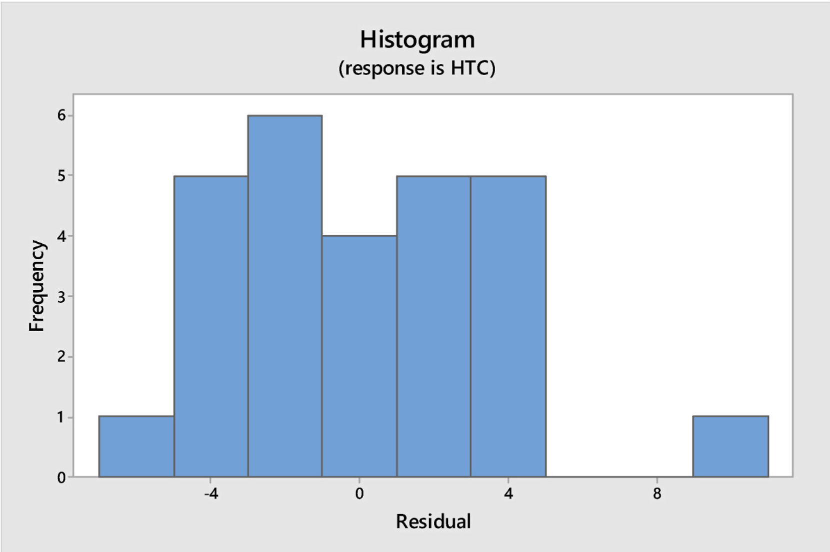

Fig. 10. Histogram of the residuals.

highest level of nozzle inclination angle (*A*), the lowest level of spray height (*H*), and the highest level of inlet water pressure (*P*).

For three independent variables against one dependent variable, interaction plots were obtained. Fig. 6 represents the interaction plots between nozzle inclination angle, water pressure, and spray height on HTC. The plot shows that the HTC decreases when spraying height increases. Also, when the water pressure and nozzle inclination angle increase, the HTC increases, but the rate of increase of the HTC with respect to the nozzle inclination angle is greater than that of water pressure. The growth rate in the HTC from 30 to 45° angle is higher than that of 45–60° angle.

The regression equation for HTC is:

$$\text{HTC} = 33.4 + 5.072{*}A - 14.6{*}H + 0.54{*}P - 0.2393{*}A{*}H + 0.0387{*}A{*}P + 0.165{*}H{*}P - 0.03160{*}A^2 + 0.79{*}H^2 + 0.0217{*}P^2 \tag{2}$$

where, *Nozzle Inclination angle* = *A*, *Spray height* = *H*, *Inlet water pressure* = *P*.

Here coefficients of *A* (nozzle inclination angle) and *P* (water pressure) are positive, indicating that the HTC increases with an increase in nozzle inclination angle and water pressure. In contrast, the coefficient of *H* (spray height) is negative, which indicates a decrease in HTC with the increase in spray height. The predictions as per Eq (2) are compared with the experimental values of HTC in

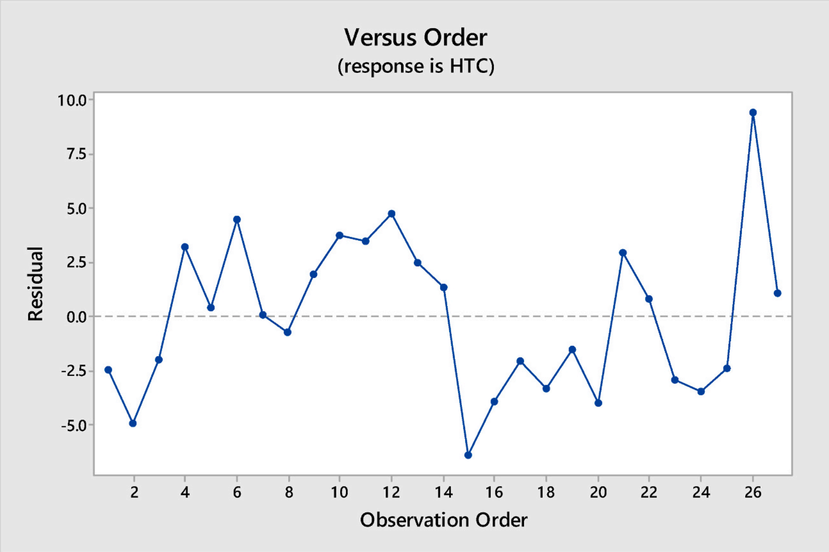

Fig. 11. Residuals vs. observations.

Fig. 7.

Fig. 8 depicts the normal probability plot of residuals as a percentage. Here the residuals of 24 observations lie closer to the Gaussian continuous normal plot, which suggests the minimum variance associated with the corresponding observations. The other three observations can be termed as outliers, bringing the regression coefficient down.

Fig. 9 shows the distribution of residuals for the 27 experimental observations. The residuals are scattered in the domain space without following any general trend, meaning the variance is minimal and uniformly distributed about the population's mean.

The histogram of the residuals is shown in Fig. 10. According to which the data fit a normal distribution curve, the skewness of the data is the least.

Fig. 11 shows the distribution of residuals vs. observations. There is no definite trend for the distribution of independent residuals, which indicates that the independent variables are not correlated, as seen from the VIF values (Table 2).

The contour plots are shown in Fig. 12. It is observed that with an increase in inclination angle and a decrease in spray height, the HTC increased (Fig. 12(a)). The HTC increased with inlet water pressure and inclination angle (Fig. 12(b)). Further, the HTC increased with an increase in inlet water pressure and a decrease in spray height (Fig. 12(c)).

The Pareto chart is shown in Fig. 13. All the independent variables are significant as they have crossed the critical value standardised effect line of 2.07. The standardised effect is nothing but a *T* value of *T* statistics, which is calculated for a degree of freedom of 26 (Table 2) and a significance level of 0.05. According to the Pareto chart, the greater the standardised effect, the more influence the intended variable should have on the performance indicator. Hence, the nozzle inclination angle has a higher effect, followed by water pressure and spray height.

3.6. S/N ratio in response

The S/N ratio ensures the presence of more helpful information than unwanted data when we select "larger is better". Table 4 summarises the response to current experimentation. This indicates that the nozzle inclination angle significantly impacts the HTC (Rank 1), followed by inlet water pressure (Rank 2). Spray height (Rank 3) was observed to have the most negligible effect among the three independent variables under study.

The main effects plots for the signal-to-noise (S/N) ratio were employed to visualise the relationship between the spray factors and the output response, namely, the heat transfer coefficient. The output of the main effects plots illustrates how parameters such as nozzle inclination angle, inlet water pressure, and spray height influence the S/N ratio. The S/N ratio was utilised to evaluate the robustness of a data set by comparing its mean value, representing the desired effect, to its standard deviation, representing the unwanted effect. The S/N ratio was used to determine the optimal value of an operating parameter. Error charts are valuable for assessing the average percentage error and interpreting its significance. If the value is sufficiently low and falls within the acceptable range, further analysis can be conducted with ease. The main effects plot of the S/N ratio (Fig. 14) indicates that nozzle inclination at 60° has the most significant impact on the S/N ratio, followed by 15 psi pressure. A spray Height of 4 cm results in most S/N ratios compared to 5 and 6 cm. On average, spray height had a negligible effect compared to the remaining two independent spray variables.

In current spray cooling experimentation, obtaining a maximum HTC was desirable, which ensures enhanced heat transfer performance. Here, optimum conditions were found as nozzle inclination angle, 60°, inlet water pressure, 15 psi, and spray height, 4 cm, to get the maximum value of HTC, 181.4 kW/m^2K.

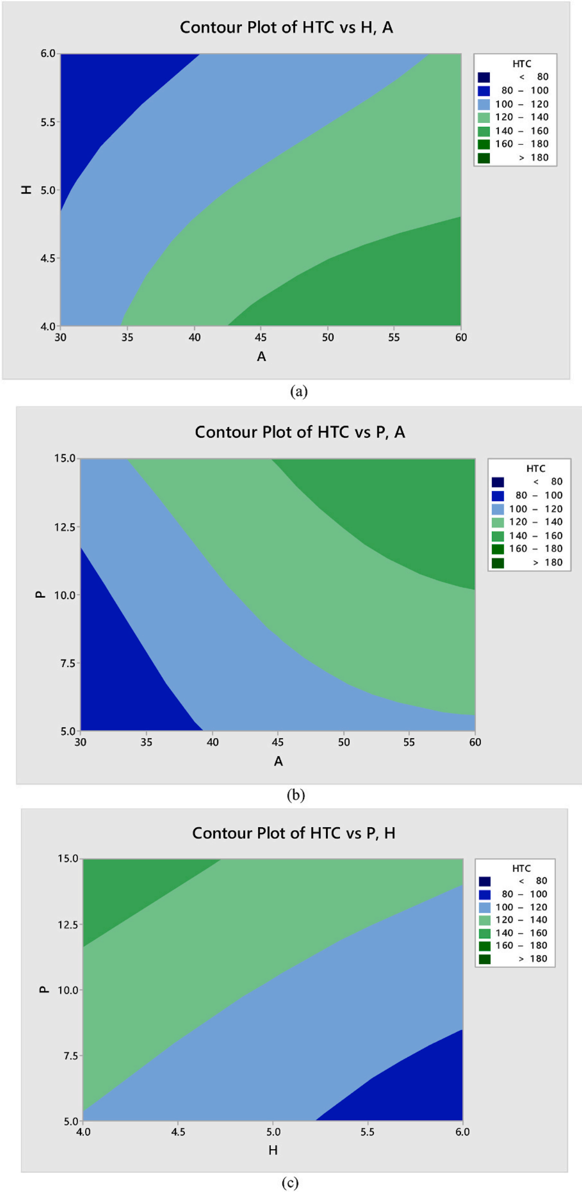

Fig. 12. Contour plots (a) effect of nozzle inclination angle and spray height (b) effect of nozzle inclination angle and water pressure, and (c) effect of spray height and water pressure on HTC.

Three outliers bring the regression coefficient down based on the normal probability plot of residuals (Fig. 8). This indicates the scope for further improvement in HTC's prediction. This has motivated us to develop the computational model for HTC's prediction. Hence, machine learning models, namely, the Random Forest and support vector machines algorithms, were used in the present study.

3.7. Random forest method

Random forest, an ensemble technique, is the most preferred Machine Learning method for solving classification and regression problems [67]. The Random Forest model comprises the decision trees that operate on small subsets of a primary data set. The random forest method does not rely on a single decision tree; instead, it takes the average of all the decision trees to get an enhanced accuracy [68,69]. The selection of a more significant number of trees in the Random Forest model avoids the problem of overfitting and also improves the accuracy [70]. In the Random Forest method, not necessarily all the decision trees are highly accurate, but the averaging of prediction of all the decision trees makes it highly accurate [71]. It is the most popular method since the training time involved is much less and maintains good accuracy even though much data is missing.

Random Forest randomly selects data points from the training dataset and constructs a decision tree for each selected point. The

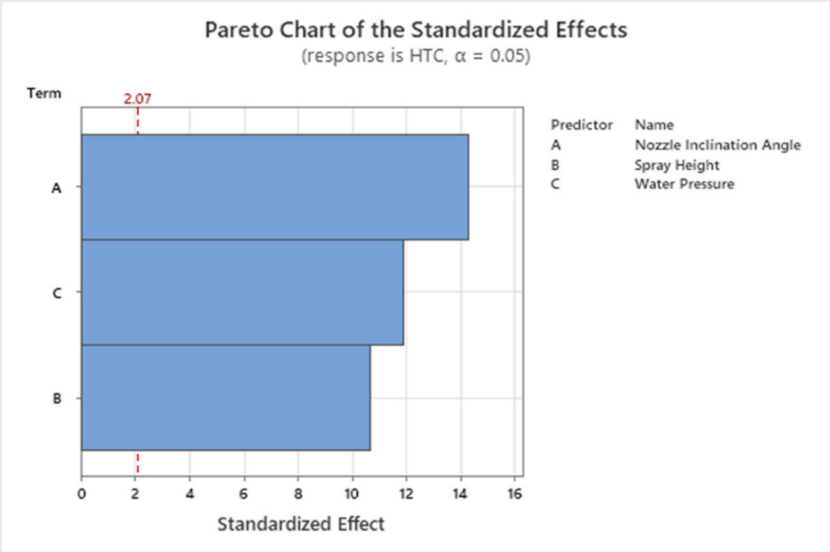

Fig. 13. Pareto chart.

Table 4
Response Table based on S/N Ratio.

Level	Nozzle inclination angle (*A*)	Spray height (*H*)	Inlet water pressure (*P*)
1	39.55	42.49	40.01
2	41.78	41.40	41.39
3	42.72	40.16	42.65
Delta	3.17	2.34	2.64
Rank	1	3	2

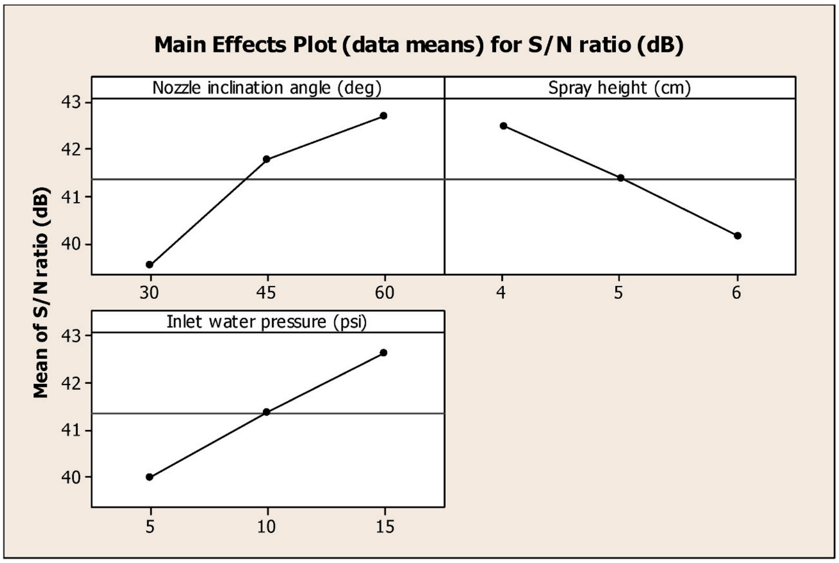

Fig. 14. Main effect plot for signal to noise ratio.

number of trees to be built is a specified parameter. For each new data point, all trees predict an output. The final output is the average of these predictions from all decision trees. The experimental data of Taguchi's L_{27} array was used to build the random forest model. The Random Forest model is implemented in Python Jupyter Notebook [72]. The number of decision trees employed in this work was 400, and the results for the corresponding model are given, as shown in Fig. 15.

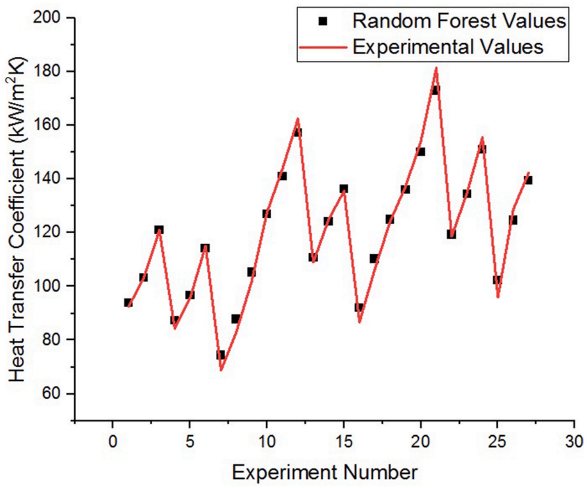

Fig. 15. Comparison plot of experimental and RFM values of HTC.

It is quite evident from Fig. 15 that the RFM values of the HTC are in good agreement with the corresponding experimental values. The maximum and average errors in the RFM predicted HTC values are 6.14 % and 2.48 %, respectively.

From Fig. 16, the RFM HTC contours for different cases do not match the experimental contours, though the average and maximum prediction errors are within an acceptable error of 6.14 %. This mismatch of contours of RFM and experimental models led to using one more machine learning model named the Support vector machine.

The percentage contribution of the spray cooling process parameters on the heat transfer coefficient, as predicted by the Random Forest algorithm, is shown in Fig. 17. According to the figure, the percentage contributions of the nozzle inclination angle, spray height, and inlet water pressure are 44.76 %, 25.15 %, and 30.08 %, respectively. The percentage contribution values predicted by the Random Forest method are in fair agreement with the ANOVA values presented in Table 2.

3.8. Support vector regression

Support Vector Regression is the most used supervised machine learning method for classification and regression problems. This technique handles the aspect of nonlinearity pretty well [73]. The support vector uses the straight-line hyperplane to fit the data. The main concept behind the support vector regression is to locate the position of a hyperplane in a high dimensional domain that classifies data points distinctly [74]. The data points nearest to the hyperplane on either side are called support. These vectors decide the orientation and position of hyperplanes. The SVR model uses Kernel's mathematical functions to convert the input data to a required form. The most used kernel mathematical functions are Linear, Polynomial, Non-linear, sigmoid and Radial basis functions. The Support vector model also uses the boundary lines at a distance epsilon from the hyperplanes to develop a margin on the data space [75]. SVR aims to find the best-fit line with the maximum count of data points.

The relation between the dependent and independent parameters in SVR is approximated by Eq. (3) [76].

$$B = f(C) = W\,x\varnothing(C) + D \tag{3}$$

B = dependent parameter, C = independent parameter, W = Weight matrix, D = model constant, $\varnothing(C)$ = high-dimensional continuum.

The minimisation of a regularised function by SVR is done as per the following equations,

Minimise:

$$S(f) = \gamma\frac{1}{P}\sum_{q=1}^{q=Q}\left(\delta_j + {\delta_j}^{*}\right) + \frac{1}{2}W^2 \tag{4}$$

Model Constraints:

$$\begin{cases} B_j - wx\varnothing(C_j) - D \le (\delta + \delta_j) \\ wx\varnothing(C_j) + D - B_i \le \delta + \delta_j^{*} \\ \delta_j, \delta_j \ge 0 \end{cases} \tag{5}$$

By employing the Lagrangian multipliers (α_j, α_j^{*}) and the kernel function $K\left(B, B_j\right)$, the solution for the above optimisation equation is given as,

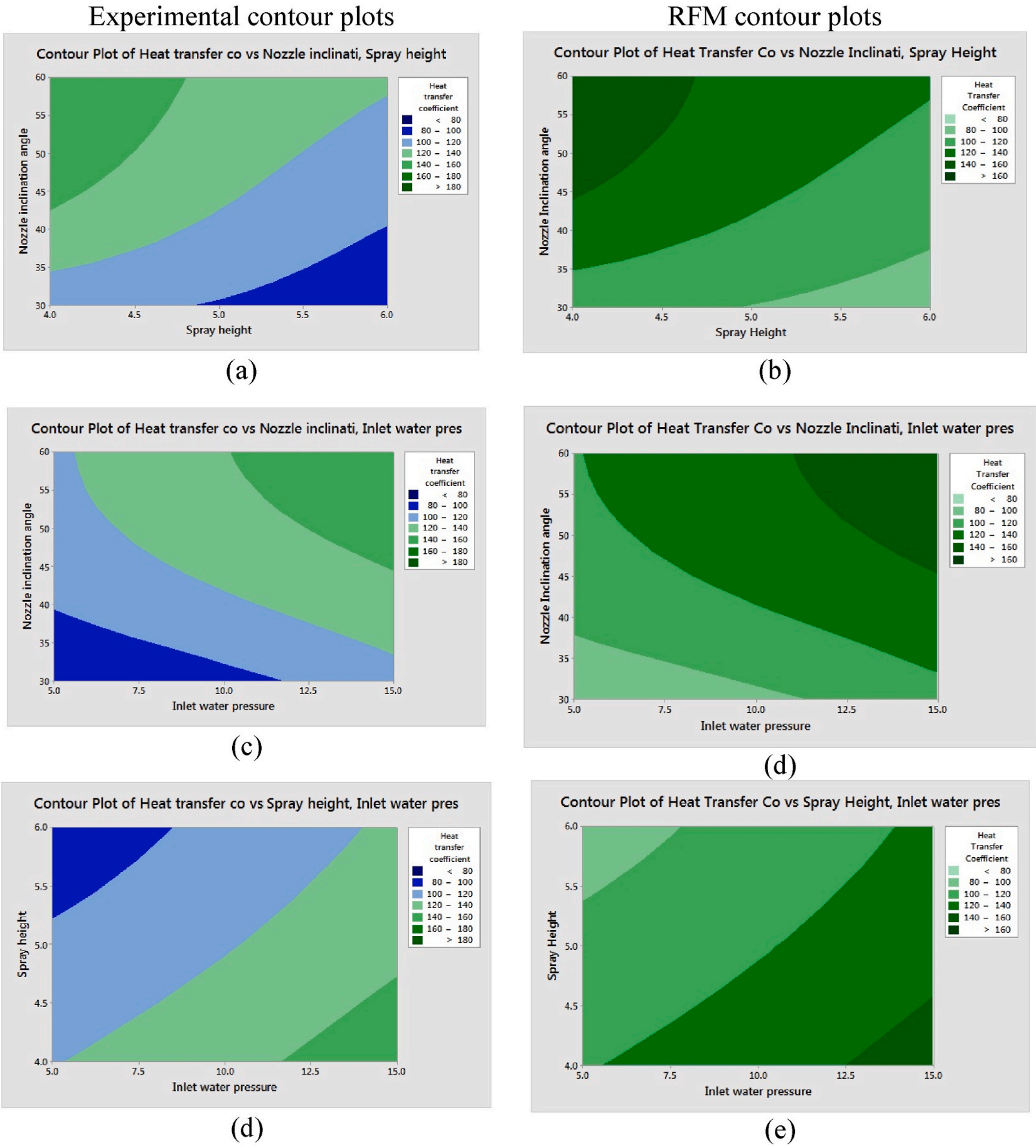

Fig. 16. Contour plots – RFM.

Maximise

$$-\frac{1}{2}\sum_{q=1}^{q=Q} 1 \sum_{L=1}^{L=m}\left(\alpha_j-\alpha_j^*\right)(\alpha_k-\alpha_k^*)K(B_j,B_k)-\varepsilon\sum_{j=1}^{j=m}\left(\alpha_j-\alpha_j^*\right)+\sum_{j=1}^{j=m}A_j\left(\alpha_j-\alpha_j^*\right) \tag{6}$$

Model Constraints:

$$\begin{cases}\sum_{q=1}^{q=Q}\left(\alpha_j-\alpha_j^*\right)=0\\ \alpha_j,\alpha_j^*\varepsilon(0,\gamma)\end{cases} \tag{7}$$

The above mentioned optimisation problem, after solving, yields the SVR equation as given below

$$B=f(C)=\left(\alpha_j-\alpha_j^*\right)xK(B,B_j)+D \tag{8}$$

The SVM algorithm is implemented in Python Jupyter Notebook using the following SVR model hyperparameters. (Table 5).

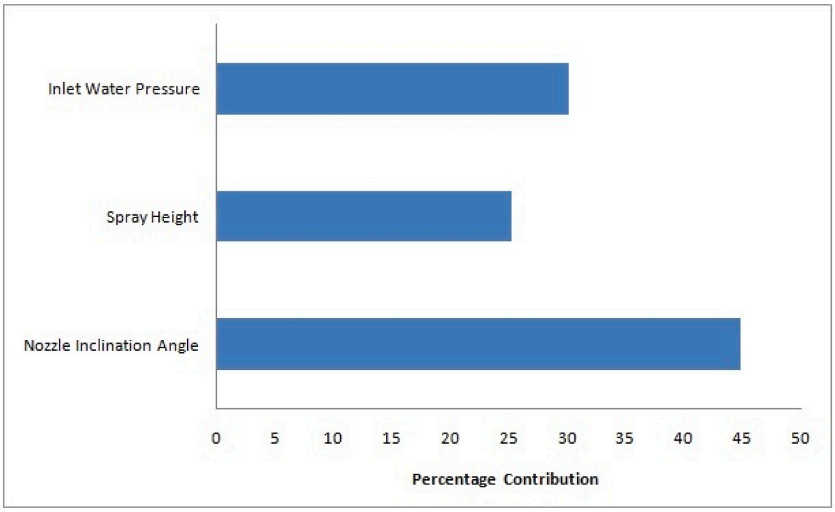

Fig. 17. Feature importance plot.

Table 5
SVR model hyperparameters.

Penalty parameter (*C*)	10000
Kernel	Radial basis function
Gamma	0.5
Epsilon	0.07

The Experimental data of Taguchi's L_{27} array was employed for training of the SVR Machine learning model. The comparison between the experimental and SVR values of HTC was made, and the results are plotted in Fig. 18.

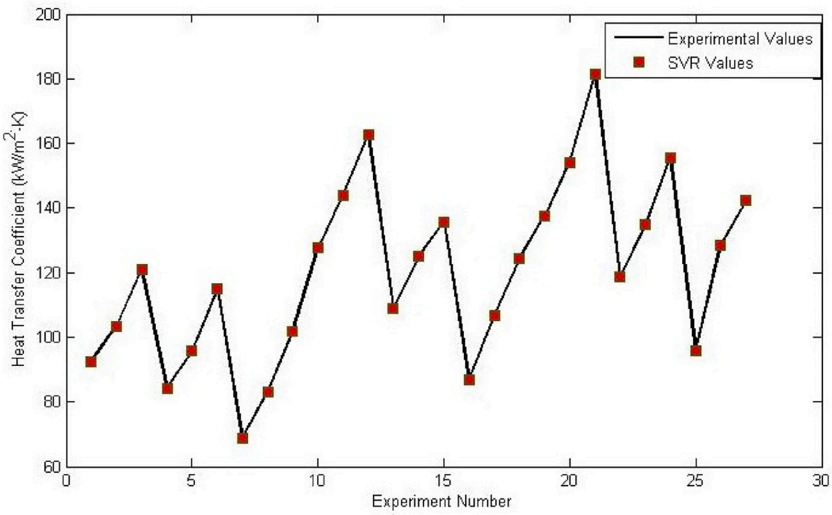

Fig. 18. Comparison plot of experimental and SVR values of HTC.

It is clear from Fig. 18 that the SVR predicted of HTCs closely match those of experimental values. The maximum and average errors in the SVR predicted HTC values are 0.15 % and 0.009 %, respectively. The SVR HTC contours for different cases match the experimental contours (Fig. 19).

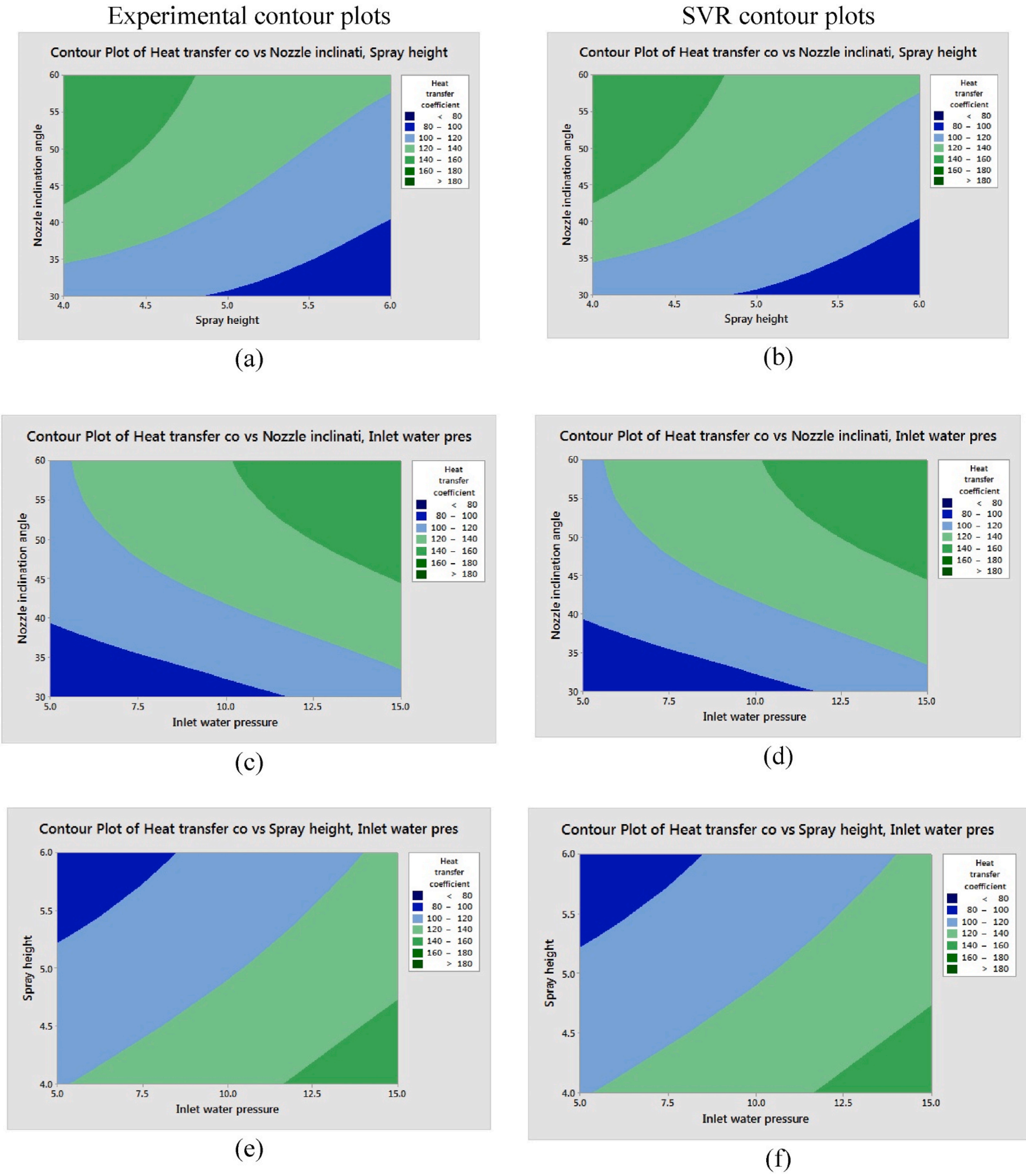

Fig. 19. Contour plots – SVR.

4. Conclusions

This study is focused on spray cooling in low heat flux regions through experimental investigations. The impact of spray variables on the heat transfer mechanism in spray cooling was discussed. An orthogonal L_{27} Taguchi array technique was used to design experiments. The ANOVA analysis tool indicates the effect of variables such as nozzle inclination angle, inlet water pressure, and spray height. This statistical analysis showed that the nozzle inclination angle in spray cooling was the variable most influencing the HTC. Results demonstrated that the optimal levels of the independent variables for achieving maximum heat transfer coefficient were A3H1P3, corresponding to the highest nozzle inclination angle, the lowest nozzle tip-to-plate height, and the highest water pressure. The relative influence of these variables on the heat transfer coefficient (HTC) was determined to be nozzle inclination angle (42.42 %) > inlet water pressure (29.31 %) > spray height (23.51 %). A maximum HTC of 181.4 kW/m^{2}K was determined at a nozzle inclination angle 60°, spray height 4 cm, and inlet water pressure of 15 psi. The machine learning models, namely random forest methods and support vector machine, yielded the maximum prediction error of 6.14 % and 0.15 %, respectively, against a prediction error of 7.24 % for the multiple regression model. Thus, a Support Vector Machine can be successfully utilised to predict the HTC for spray cooling heat transfer.

Plate 1. Photograph of the experimental test rig.

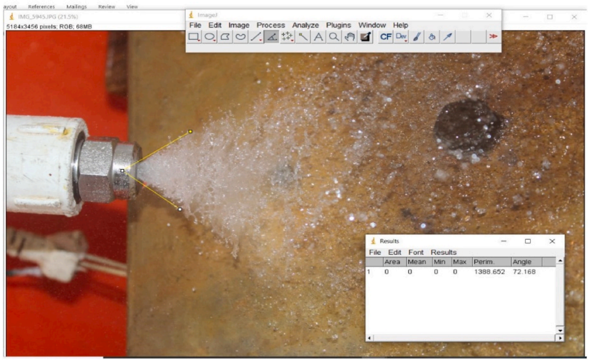

Plate 2. Photograph of the velocity distribution of the spray.

CRediT authorship contribution statement

Umesh B. Deshannavar: Writing – original draft, Formal analysis, Data curation. **Saee H. Thakur:** Visualization, Validation, Investigation. **Amith H. Gadagi:** Visualization, Validation, Investigation. **Santosh A. Kadapure:** Visualization, Validation, Investigation. **Santhosh Paramasivam:** Writing – review & editing, Validation, Data curation, Formal analysis, Conceptualization. **Natarajan Rajamohan:** Writing – review & editing, Validation, Supervision, Project administration, Conceptualization. **Raffaello Possidente:** Visualization, Writing – review & editing, Validation. **Gianluca Gatto:** Validation, Supervision, Funding acquisition, Project administration, Writing – review & editing.

Data availability

Data and materials are available with the authors and can be reproduced in case of its need.

Funding details

This research was also partially funded within Project AISAC (Analisi e Ingegnerizzazione dei Sistemi Alimentari Complessi) by Italian Government (Ministero delle Imprese e del Made in Italy), Fondo per la Crescita Sostenibile - Accordi per l'innovazione di cui al D.M. 31 dicembre 2021 e D.D. 18 marzo 2022, grant no. F/310035/05/X56.

Declaration of competing interest

The authors declare that they have no known competing financial interests or personal relationships that could have appeared to influence the work reported in this paper.

Data availability

The authors do not have permission to share data.

References

[1] R. Kumar, R. Nadda, S. Kumar, S. Saboor, C. Ahamed Saleel, M. Abbas, A. Afzal, E. Linul, Convective heat transfer enhancement using impingement jets in channels and tubes: a comprehensive review, Alex. Eng. J. 70 (2023) 349–376, https://doi.org/10.1016/j.aej.2023.02.013.

[2] N. Uddin, P.T.W. Kee, B. Weigand, Heat transfer by jet impingement: a review of heat transfer correlations and high-fidelity simulations, Appl. Therm. Eng. 257 (2024) 124258, https://doi.org/10.1016/j.applthermaleng.2024.124258.

[3] A. Labergue, M. Gradeck, F. Lemoine, Comparative study of the cooling of a hot temperature surface using sprays and liquid jets, Int. J. Heat Mass Tran. 81 (2015) 889–900, https://doi.org/10.1016/j.ijheatmasstransfer.2014.11.018.

[4] W.L. Cheng, W.W. Zhang, H. Chen, L. Hu, Spray cooling and flash evaporation cooling: the current development and application, Renew. Sustain. Energy Rev. 55 (2016) 614–628, https://doi.org/10.1016/j.rser.2015.11.014.

[5] J. Kim, Spray cooling heat transfer: the state of the art, Int. J. Heat Fluid Flow 28 (2007) 753–767, https://doi.org/10.1016/j.ijheatfluidflow.2006.09.003.

[6] N. Liu, L. Li, Y.T. Kang, Experimental study on heat transfer performance enhancement by micro-structured surfaces for inclination spray application, Int. J. Heat Mass Tran. 133 (2019) 631–640, https://doi.org/10.1016/j.ijheatmasstransfer.2018.12.177.

[7] P. Smakulski, J. Ishimoto, S. Pietrowicz, The cooling performance of the micro-solid nitrogen spray technique on the cryopreservation vitrification process: a qualitative study, Int. J. Heat Mass Tran. 184 (2022) 122253, https://doi.org/10.1016/J.IJHEATMASSTRANSFER.2021.122253.

[8] P. GaneshKumar, V. Sivalingam, V.S. Vigneswaran, V. Ramalingam, K. Seong Cheol, R. Vanaraj, Spray cooling for hydrogen vehicle, electronic devices, solar and building (low temperature) applications: a state-of-art review, Renew. Sustain. Energy Rev. 189 (2024) 113931, https://doi.org/10.1016/j.rser.2023.113931.

[9] C. Wang, Q. Lu, Y. Liu, H. Huang, J. Sun, Progressive review of heat transfer enhancement technologies in 2010–2020, Sustain. Energy Technol. Assessments 56 (2023) 103121, https://doi.org/10.1016/j.seta.2023.103121.

[10] Y.-G. Lv, Y.-T. Wang, T. Meng, Q.-W. Wang, W.-X. Chu, Review on thermal management technologies for electronics in spacecraft environment, Energy Storage and Saving 3 (2024) 153–189, https://doi.org/10.1016/j.enss.2024.03.001.

[11] K.Y.M. Almajhali, Review on passive energy dissipation devices and techniques of installation for high rise building structures, Structures 51 (2023) 1019–1029, https://doi.org/10.1016/j.istruc.2023.03.025.

[12] I. Vladyko, N. Miskiv, K. Pavlenko, A. Chernyavskiy, A. Surtaev, Heat transfer peculiarities and crisis phenomena development in spray cooling using various types of nozzles, Int. Commun. Heat Mass Tran. 159 (2024) 108145, https://doi.org/10.1016/j.icheatmasstransfer.2024.108145.

[13] X. Liu, C. Du, J. Zhu, H. Kang, C. Ding, Numerical investigation of liquid nitrogen spray cooling under low ambient pressure, Int. J. Heat Mass Tran. 233 (2024) 126048, https://doi.org/10.1016/j.ijheatmasstransfer.2024.126048.

[14] G. Liang, I. Mudawar, Review of spray cooling – Part 1: single-phase and nucleate boiling regimes, and critical heat flux, Int. J. Heat Mass Tran. 115 (2017) 1174–1205, https://doi.org/10.1016/j.ijheatmasstransfer.2017.06.029.

[15] A. Labergue, M. Gradeck, F. Lemoine, Comparative study of the cooling of a hot temperature surface using sprays and liquid jets, Int. J. Heat Mass Tran. 81 (2015) 889–900, https://doi.org/10.1016/j.ijheatmasstransfer.2014.11.018.

[16] H. Wan, P.J. Liu, G.Q. He, Z.R. Xue, F. Qin, W.Q. Li, Experimental and numerical studies on the spray cooling of deionized water in non-boiling regime, Case Stud. Therm. Eng. 44 (2023) 102834, https://doi.org/10.1016/j.csite.2023.102834.

[17] P. Tan, X. Liu, B. Cao, W. Chen, J. Feng, Z. Xiang, Experimental study on heat transfer performance of high-power spray cooling system based on multi-factor orthogonal test, Case Stud. Therm. Eng. 49 (2023) 103287, https://doi.org/10.1016/j.csite.2023.103287.

[18] I. Vladyko, N. Miskiv, K. Pavlenko, A. Chernyavskiy, A. Surtaev, Heat transfer peculiarities and crisis phenomena development in spray cooling using various types of nozzles, Int. Commun. Heat Mass Tran. 159 (2024) 108145, https://doi.org/10.1016/j.icheatmasstransfer.2024.108145.

[19] J.L. Xie, Y.B. Tan, T.N. Wong, F. Duan, K.C. Toh, K.F. Choo, P.K. Chan, Y.S. Chua, Multi-nozzle array spray cooling for large area high power devices in a closed loop system, Int. J. Heat Mass Tran. 78 (2014) 1177–1186, https://doi.org/10.1016/j.ijheatmasstransfer.2014.07.067.

[20] Y. Hou, J. Liu, X. Su, Y. Qian, L. Liu, X. Liu, Experimental study on the characteristics of a closed loop R134-a spray cooling, Exp. Therm. Fluid Sci. 61 (2015) 194–200, https://doi.org/10.1016/j.expthermflusci.2014.10.026.

[21] K. Zhao, Y. Jiang, Y. Wang, F. Zhu, Y.-Z. Xu, H. Wu, Experimental research on heat transfer characteristics of spray cooling under swing excitation, Appl. Therm. Eng. 255 (2024) 123947, https://doi.org/10.1016/j.applthermaleng.2024.123947.

[22] Z.-F. Zhou, R. Wang, B. Chen, T. Yang, G.-X. Wang, Heat transfer characteristics during pulsed spray cooling with R404A at different spray distances and back pressures, Appl. Therm. Eng. 102 (2016) 813–821, https://doi.org/10.1016/j.applthermaleng.2016.04.004.

[23] Y. Zhao, S. Gong, G. Zhang, Y. Wang, M. Ge, Experimental study of heat transfer characteristics and energy consumption of spray cooling, Energy Rep. 8 (2022) 271–276, https://doi.org/10.1016/j.egyr.2022.10.255.

[24] J. Chen, X. Liu, F. Zhong, Q. Miao, W. Jia, M. Zheng, Y. Li, Y. Hou, Experimental study of dielectric liquid spray cooling on multi-scale structured surfaces inspired by leaf veins, Int. J. Heat Fluid Flow 109 (2024) 109554, https://doi.org/10.1016/j.ijheatfluidflow.2024.109554.

[25] S. Qin, R. Ji, C. Miao, L. Jin, C. Yang, X. Meng, Review of enhancing boiling and condensation heat transfer: surface modification, Renew. Sustain. Energy Rev. 189 (2024) 113882, https://doi.org/10.1016/j.rser.2023.113882.

[26] J.L. Xie, Y.B. Tan, F. Duan, K. Ranjith, T.N. Wong, K.C. Toh, K.F. Choo, P.K. Chan, Study of heat transfer enhancement for structured surfaces in spray cooling, Appl. Therm. Eng. 59 (2013) 464–472, https://doi.org/10.1016/j.applthermaleng.2013.05.047.

[27] A.G. Ulson de Souza, J.R. Barbosa, Experimental evaluation of spray cooling of R-134a on plain and enhanced surfaces, Int. J. Refrig. 36 (2013) 527–533, https://doi.org/10.1016/j.ijrefrig.2012.11.028.

[28] L. Xiang, X. Yu, T. Hong, X. Yang, B. Xie, R. Hu, X. Luo, Performance of spray cooling with vertical surface orientation: an experimental investigation, Appl. Therm. Eng. 219 (2023) 119434, https://doi.org/10.1016/j.applthermaleng.2022.119434.

[29] H.-T. Chen, H.-C. Lee, Estimation of spray cooling characteristics on a hot surface using the hybrid inverse scheme, Int. J. Heat Mass Tran. 50 (2007) 2503–2513, https://doi.org/10.1016/j.ijheatmasstransfer.2006.12.021.

[30] S.Y. Lee, T.W. Huang, Inverse analysis of spray cooling on a hot surface with experimental data, Int. J. Therm. Sci. 100 (2016) 145–154, https://doi.org/10.1016/j.ijthermalsci.2015.09.020.

[31] I. Vladyko, N. Miskiv, K. Pavlenko, A. Chernyavskiy, A. Surtaev, Heat transfer peculiarities and crisis phenomena development in spray cooling using various types of nozzles, Int. Commun. Heat Mass Tran. 159 (2024) 108145, https://doi.org/10.1016/j.icheatmasstransfer.2024.108145.

[32] Y. Wang, Y. Jiang, W. Chen, B. Zhou, Heat transfer characteristics of spray cooling beyond critical heat flux under severe heat dissipation condition, Appl. Therm. Eng. 123 (2017) 1356–1364, https://doi.org/10.1016/j.applthermaleng.2017.04.165.

[33] Y.T. Aksoy, Y. Zhu, P. Eneren, E. Koos, M.R. Vetrano, The impact of nanofluids on droplet/spray cooling of a heated surface: a critical review, Energies 14 (2021) 1–34, https://doi.org/10.3390/en14010080.

[34] W.L. Cheng, Q.N. Liu, R. Zhao, H.L. Fan, Experimental investigation of parameters effect on heat transfer of spray cooling, Heat and Mass Transfer/Waerme-Und Stoffuebertragung 46 (2010) 911–921, https://doi.org/10.1007/s00231-010-0631-5.

[35] X. Gao, R. Li, Effects of nozzle positioning on single-phase spray cooling, Int. J. Heat Mass Tran. 115 (2017) 1247–1257, https://doi.org/10.1016/j.ijheatmasstransfer.2017.08.095.

[36] A.S. Salman, T.C. Paul, J.A. Khan, The effects of coverage area on the spray cooling heat transfer performance, in: Proceedings of the Thermal and Fluids Engineering Summer Conference 2018, 2018, pp. 1345–1353, https://doi.org/10.1615/TFEC2018.hte.021183. March.

[37] A.S. Salman, N.M. Abdulrazzaq, A. Tikadar, S.K. Oudah, J.A. Khan, Parametric study of heat transfer characteristics of enhanced surfaces in a spray cooling system: an experimental investigation, Appl. Therm. Eng. 183 (2021) 115824, https://doi.org/10.1016/j.applthermaleng.2020.115824.

[38] M.R. Pais, L.C. Chow, E.T. Mahefkey, Surface roughness and its effects on the heat transfer mechanism in spray cooling, J. Heat Tran. 114 (1992) 211–219, https://doi.org/10.1115/1.2911248.

[39] N. Zhou, F. Chen, Y. Cao, M. Chen, Y. Wang, Experimental investigation on the performance of a water spray cooling system, Appl. Therm. Eng. 112 (2017) 1117–1128, https://doi.org/10.1016/j.applthermaleng.2016.10.191.

[40] H. Liu, C. Cai, Y. Yan, M. Jia, B. Yin, Numerical simulation and experimental investigation on spray cooling in the non-boiling region, Heat and Mass Transfer/ Waerme- Und Stoffuebertragung 54 (2018) 3747–3760, https://doi.org/10.1007/s00231-018-2402-7.

[41] W.-L. Cheng, F.-Y. Han, Q.-N. Liu, H.-L. Fan, Spray characteristics and spray cooling heat transfer in the non-boiling regime, Energy 36 (2011) 3399–3405, https://doi.org/10.1016/j.energy.2011.03.039.

[42] S.K. Nayak, P.C. Mishra, S.K.S. Parashar, Influence of spray characteristics on heat flux in dual phase spray impingement cooling of hot surface, Alex. Eng. J. 55 (2016) 1995–2004, https://doi.org/10.1016/j.aej.2016.07.015.

[43] M. Aamir, Q. Liao, Z. Xun, Aqeel-Ur Rehman, W. Hong, M. Zubair, Estimation of surface heat flux and surface temperature during inverse heat conduction under varying spray parameters and sample initial temperature, Sci. World J. 2014 (2014), https://doi.org/10.1155/2014/721620.

[44] H. Mzad, R. Khelif, Effect of spraying pressure on spray cooling enhancement of beryllium-copper alloy plate, Procedia Eng. 157 (2016) 106–113, https://doi.org/10.1016/j.proeng.2016.08.344.

[45] S. Thakur, S. Kadapure, P. Hegde, U. Deshannavar, A review of parameters and mechanisms in spray cooling, J. Inst. Eng. 29 (2023) 36–64, https://doi.org/10.56801/MME1016.

[46] M. Hnizdil, M. Chabicovsky, M. Raudensky, T. Lee, Heat Transfer during Spray Cooling.Pdf, 2016, pp. 104–113.

[47] M. Aamir, Q. Liao, Z. Xun, Aqeel-Ur Rehman, W. Hong, M. Zubair, Estimation of surface heat flux and surface temperature during inverse heat conduction under varying spray parameters and sample initial temperature, Sci. World J. 2014 (2014), https://doi.org/10.1155/2014/721620.

[48] F.V. Barbosa, S.D.T. Sousa, S.F.C.F. Teixeira, J.C.F. Teixeira, Application of Taguchi method for the analysis of a multiple air jet impingement system with and without target plate motion, Int. J. Heat Mass Tran. 176 (2021) 121504, https://doi.org/10.1016/j.ijheatmasstransfer.2021.121504.

[49] H. Mzad, R. Khelif, Effect of spraying pressure on spray cooling enhancement of beryllium-copper alloy plate, Procedia Eng. 157 (2016) 106–113, https://doi.org/10.1016/j.proeng.2016.08.344.

[50] W.L. Cheng, F.Y. Han, Q.N. Liu, H.L. Fan, Spray characteristics and spray cooling heat transfer in the non-boiling regime, Energy 36 (2011) 3399–3405, https://doi.org/10.1016/j.energy.2011.03.039.

[51] A.S. Salman, J.A. Khan, The effects of spraying parameters on spray cooling heat transfer, in: Proceedings of the ASME 2017 International Mechanical Engineering Congress and Exposition, 2017, pp. 1–8.

[52] Y. Cheng, F. Wang, J. Xu, D. Liu, Y. Sui, Numerical investigation of droplet spreading and heat transfer on hot substrates, Int. J. Heat Mass Tran. 121 (2018) 402–411, https://doi.org/10.1016/j.ijheatmasstransfer.2018.01.026.

[53] Z.B. Yan, K.C. Toh, F. Duan, T.N. Wong, K.F. Choo, P.K. Chan, Y.S. Chua, Experimental study of impingement spray cooling for high power devices, Appl. Therm. Eng. 30 (2010) 1225–1230, https://doi.org/10.1016/j.applthermaleng.2010.02.003.

[54] H. Liu, C. Cai, Y. Yan, M. Jia, B. Yin, Numerical simulation and experimental investigation on spray cooling in the non-boiling region, Heat and Mass Transfer/ Waerme- Und Stoffuebertragung 54 (2018) 3747–3760, https://doi.org/10.1007/s00231-018-2402-7.

[55] W.L. Cheng, Q.N. Liu, R. Zhao, H.L. Fan, Experimental investigation of parameters effect on heat transfer of spray cooling, Heat and Mass Transfer/Waerme-Und Stoffuebertragung 46 (2010) 911–921, https://doi.org/10.1007/s00231-010-0631-5.

[56] R. Zhao, W. Cheng, Q. Liu, H. Fan, Study on heat transfer performance of spray cooling: model and analysis, Heat Mass Tran. 46 (2010) 821–829, https://doi.org/10.1007/s00231-010-0632-4.

[57] W.-L. Cheng, Q.-N. Liu, R. Zhao, H. Fan, Experimental investigation of parameters effect on heat transfer of spray cooling, Heat Mass Tran. 46 (2010) 911–921, https://doi.org/10.1007/s00231-010-0631-5.

[58] Y.B. Tan, J.L. Xie, F. Duan, T.N. Wong, K.C. Toh, K.F. Choo, P.K. Chan, Y.S. Chua, Multi-nozzle spray cooling for high heat flux applications in a closed loop system, Appl. Therm. Eng. 54 (2013) 372–379, https://doi.org/10.1016/j.applthermaleng.2013.01.033.

[59] Y. Tao, X. Huai, L. Wang, Z. Guo, Experimental characterization of heat transfer in non-boiling spray cooling with two nozzles, Appl. Therm. Eng. 31 (2011) 1790–1797, https://doi.org/10.1016/j.applthermaleng.2011.02.025.

[60] A.S. Salman, T.C. Paul, J.A. Khan, The effects of coverage area on the spray cooling heat transfer performance, in: Proceedings of the Thermal and Fluids Engineering Summer Conference 2018, 2018, pp. 1345–1353, https://doi.org/10.1615/TFEC2018.hte.021183. March.

[61] J. Tian, B. Chen, Z. Zhou, D. Li, Theoretical study on cryogen spray cooling in laser treatment of ota's nevus: comparison and optimization of R134a, R404A and R32, Energies 13 (2020) 5647, https://doi.org/10.3390/en13215647.

[62] J. Yin, S. Wang, X. Sang, Z. Zhou, B. Chen, P. Thrassos, A. Romeos, A. Giannadakis, Spray cooling as a high-efficient thermal management solution: a review, Energies 15 (2022) 8547, https://doi.org/10.3390/en15228547.

[63] P. Zhang, L. Ruan, Experimental study on two-phase spray cooling for the cooling of high-heat-flux electronic chip, in: Proceedings - 2012 International Conference on Computer Distributed Control and Intelligent Environmental Monitoring, CDCIEM 2012, 2012, pp. 324–326, https://doi.org/10.1109/CDCIEM.2012.83.

[64] Y. Wang, M. Liu, D. Liu, K. Xu, Y. Chen, Experimental study on the effects of spray inclination on water spray cooling performance in non-boiling regime, Exp. Therm. Fluid Sci. 34 (2010) 933–942, https://doi.org/10.1016/j.expthermflusci.2010.02.010.

[65] X. Gao, R. Li, Effects of nozzle positioning on single-phase spray cooling, Int. J. Heat Mass Tran. 115 (2017) 1247–1257, https://doi.org/10.1016/j.ijheatmasstransfer.2017.08.095.

[66] H. Yang, X. Cao, X. Sun, Effects of spray angle on spray cooling of extruded aluminum alloy plate, AASRI Procedia 3 (2012) 630–635, https://doi.org/10.1016/j.aasri.2012.11.100.

[67] A. Chaitanya Kumar, J. Andrew John, M. Raja, P. Vijaya, Genetic factor analysis for an early diagnosis of autism through machine learning, in: Data Science for Genomics, Elsevier, 2023, pp. 69–84, https://doi.org/10.1016/B978-0-323-98352-5.00001-X.

[68] J. Wang, R.X. Gao, Innovative smart scheduling and predictive maintenance techniques, in: Design and Operation of Production Networks for Mass Personalization in the Era of Cloud Technology, Elsevier, 2022, pp. 181–207, https://doi.org/10.1016/B978-0-12-823657-4.00007-5.

[69] R.P. Selvam, Computational modeling of spray cooling: current status and future challenges, in: AIP Conf Proc, AIP, 2005, pp. 55–63, https://doi.org/10.1063/1.1867118.

[70] G. Biau, E. Scornet, A random forest guided tour, Test 25 (2016) 197–227, https://doi.org/10.1007/s11749-016-0481-7.

[71] T.P. Carvalho, F.A.A.M.N. Soares, R. Vita, R. da P. Francisco, J.P. Basto, S.G.S. Alcalá, A systematic literature review of machine learning methods applied to predictive maintenance, Comput. Ind. Eng. 137 (2019) 106024, https://doi.org/10.1016/j.cie.2019.106024.

[72] V. Dubey, A.K. Sharma, D.Y. Pimenov, Prediction of surface roughness using machine learning approach in MQL turning of AISI 304 steel by varying nanoparticle size in the cutting fluid, Lubricants 10 (2022) 81, https://doi.org/10.3390/lubricants10050081.

[73] D. Marneni, S. Vemula, Analysis of Covid-19 using machine learning techniques, in: Statistical Modeling in Machine Learning, Elsevier, 2023, pp. 37–53, https://doi.org/10.1016/B978-0-323-91776-6.00006-3.

[74] R. Gove, J. Faytong, in: Machine Learning and Event-Based Software Testing: Classifiers for Identifying Infeasible GUI Event Sequences, 2012, pp. 109–135, https://doi.org/10.1016/B978-0-12-396535-6.00004-1.

[75] M. Reza Keyvanpour, M.B. Shirzad, Machine learning techniques for agricultural image recognition, in: Application of Machine Learning in Agriculture, Elsevier, 2022, pp. 283–305, https://doi.org/10.1016/B978-0-323-90550-3.00011-4.

[76] C. Ji, F. Ma, J. Wang, W. Sun, in: Early Identification of Abnormal Deviations in Nonstationary Processes by Removing Non- Stationarity, 2022, pp. 1393–1398, https://doi.org/10.1016/B978-0-323-85159-6.50232-3.